Femtosecond spin-state photo-switching dynamics in an FeIII spin crossover solid accompanied by coherent structural vibrations

Roman Bertoni, Maciej Lorenc, Jerome Laisney, Antoine Tissot, Alain Moréac, Samir F. Matar, Marie-Laure Boillot, Eric Collet

▶ **To cite this version:**

Roman Bertoni, Maciej Lorenc, Jerome Laisney, Antoine Tissot, Alain Moréac, et al.. Femtosecond spin-state photo-switching dynamics in an FeIII spin crossover solid accompanied by coherent structural vibrations. Journal of Materials Chemistry C, 2015, 3 (30), pp.7792-7801. 10.1039/C5TC00854A . hal-01152947

HAL Id: hal-01152947
https://hal.science/hal-01152947

Submitted on 20 May 2015

HAL is a multi-disciplinary open access archive for the deposit and dissemination of scientific research documents, whether they are published or not. The documents may come from teaching and research institutions in France or abroad, or from public or private research centers.

L'archive ouverte pluridisciplinaire **HAL**, est destinée au dépôt et à la diffusion de documents scientifiques de niveau recherche, publiés ou non, émanant des établissements d'enseignement et de recherche français ou étrangers, des laboratoires publics ou privés.

Femtosecond spin-state photo-switching dynamics in an Fe^{III} spin crossover solid accompanied by coherent structural vibrations

R. Bertoni,[a] M. Lorenc,[a] J. Laisney[b], A. Tissot[b,†], A. Moréac[a], S. F. Matar[c], M.-L. Boillot[b] and E. Collet[a,*]

We investigate light-induced excited spin-state trapping (LIESST) dynamics of an Fe^{III} spin-crossover material from low (S=1/2) to high (S=5/2) spin states. Our results show that this process occurs only at the molecular level as evidenced by the linear dependence of the fraction of photo-switched molecules with the excitation density as well as with the initial fraction of low spin molecules. The inter-system crossing from photoexcited LS (S=1/2) to HS (S=5/2) occurs within ≈200 fs and is accompanied by coherent non-equilibrium vibrational relaxation in the photo-induced HS state. These results reveal similar dynamical features to those already reported for LIESST in Fe^{II} systems. The activation of coherent molecular vibrations is essential for reaching rapidly the HS potential on the timescale of molecular motions, whereas their fast damping allows an efficient trapping in the HS potential. The observed coherent oscillations are attributed to photoinduced molecules in the HS states, as supported by Raman spectroscopy at thermal equilibrium, and DFT analyses of molecular vibrations and TD-DFT calculations of optical absorption.

Introduction

In molecular science, light is known to be an efficient trigger for driving chemical reactions, breaking bonds or changing electronic molecular states[1]. Reaction coordinates connecting initial, photoexcited, and final photoinduced states are not simple to describe. Furthermore, the pathway followed on the potential energy surface is complex and numerous studies investigated how fast such processes are and how interconversion of molecular states proceeds. In the solid state too, light can switch molecules between different electronic states. Charge-transfer processes induced by light can lead to photo-induced phase transition from insulating to metallic[2] or from neutral to ionic[3] phases for example. Spin-crossover (SCO) materials are bistable molecular systems able to switch between low spin (LS) and high spin (HS) states under the effect of different control parameters such as temperature or pressure[4]. They are also prototype photoactive systems as they can be interconverted through the light-induced excited spin-state trapping (LIESST) process from LS to HS state or conversely from HS to LS state (reverse-LIESST). LIESST in crystals was discovered more than thirty years ago[5]: by irradiating SCO solids with *cw* light at low temperature complete conversion of molecular states can be generated at the macroscopic scale of the material and the photo-induced state can be metastable up to a critical temperature referred to as T(LIESST)[6]. In crystals, molecules may respond cooperatively to light excitation[2,3]. In addition, light can control order between the individual molecules of the materials and generate new phases which cannot be reached at thermal equilibrium[7]. This underlines the ability of molecular-based materials to show response to light different from the response of the individual constituting molecules. There are also other examples in the literature of molecular materials showing cooperative response to light excitation, for which a single photon transforms several molecules and the response of the molecular material is more than the sum of individual molecular events[2,3]. Spin-crossover has become a topical research area over the last three decades, with many research groups contributing to its advancement[4]. The very high efficiency and speed of the photo-induced spin state switching between two states that completely differ in physical properties (color, volume, magnetic susceptibility) represent a conceptual challenge[8]. For Fe^{II} systems the role of ligand-field states was deeply investigated[9]. The study of reverse-LIESST revealed a mechanism involving two main inter-system crossing (ISC) and therefore true intermediate electronic states (such as S=1) between the photoexcited HS (S=2) and the photoinduced LS (S=0) state, which is reached within 40 ps. But for LIESST, the irradiation into metal–ligand charge transfer (MLCT) or d-d bands of S=0 species promotes the system to the S=2 state within ≈160 fs. This timescale was determined with ultrafast optical spectroscopy, a powerful technique for investigating the photo-physical dynamics of

[a] *Institut de Physique de Rennes, Université de Rennes1, UMR UR1-CNRS 6251, F-35000 Rennes, France.*
[b] *Institut de Chimie Moléculaire et des Matériaux d'Orsay, Université Paris-Sud, UMR-CNRS 8182, Orsay, France.*
[c] *CNRS, Université de Bordeaux, ICMCB, 87 avenue du Dr. A. Schweitzer, Pessac, 33608 France.*
* Corresponding author Email address: eric.collet@univ-rennes1.fr
† Present address: Institut Lavoisier de Versailles, UMR CNRS 8180, Université de Versailles Saint-Quentin, 78035 Versailles cedex, France.
Electronic Supplementary Information (ESI) available: Videos of the molecular vibrational modes calculated at 56 cm^{-1}, 33cm^{-1} and 88 cm^{-1}.

SCO compounds[10]. Complementary ultrafast X-ray absorption spectroscopy studies revealed the structural dynamics related to ligand-cage dilation, which leads to the structural trapping of the newly formed HS electronic state[11]. On the pathway from MLCT to HS states, other not structurally relaxed electronic states serve as intermediates. Indeed, these states are populated on a timescale shorter than an oscillation period in the potential[12].

For better understanding this process, it seems necessary to track the electronic and structural pathway followed by the system with the time resolution of elementary electronic and molecular events. Recent theoretical works suggested that such speed and efficiency of LIESST results from the instantaneous activation of molecular phonons after photo-excitation[13]. This is due to the important displacive nature of the inter-system crossing, which moves the system rapidly into the HS potential with a ≈0.2 Å elongation of Fe-N bonds. The experimental proof of such a conjecture was reported recently for an Fe^{II} system[14]. This study revealed that the structural molecular reorganization, trapping the photoinduced electronic state, occurs in a two-step sequence: the molecule elongates first (within 170 femtosecond) and bends afterwards, via a coherent vibrational energy transfer between these two main structural modes.

There are very few Fe^{III} materials showing efficient or long-lived LIESST[15] but we evidenced in several SCO archetypes[16,17] by time-resolved spectroscopy that transient Fe^{III} HS state can be generated. This is also the case of the Fe^{III} SCO [Fe(3-MeO-SalEen)]PF_6 material studied here in the form of nanocrystals (average size, 900(230)×285(65)×64(18) nm^3)[8a]. Here we show that the spin-state photo-switching dynamics in this Fe^{III} material occurs locally and that the structural trapping during LIESST is accompanied by coherent molecular dynamics.

Results and discussion

Thermal spin conversion.

The Fe^{III} complex [Fe(3-MeO-SalEen)$_2$]PF_6 was originally synthesized by Hendrickson[18]. H-3-MeO-SalEen is the condensation product of 3-methoxy-substituted salicylaldehyde and N-ethyl-ethylenediamine. This Fe^{III} system can switch under the effect of external parameter, such as temperature, between LS and HS states. Since the HOMO and LUMO orbitals have a strong d character, the two electronic states correspond to:

- a low spin one (LS) with S= 1/2 with an electronic configuration $t_{2g}^5\ e_g^0$ in the octahedral-like description. More rigorously, in the symmetry of the complex the electronic configuration is $d_\pi^5\ d_\sigma^0$.
- a high spin one (HS) with S= 5/2 corresponding to the electronic configuration $t_{2g}^3\ e_g^2$ (or $d_\pi^3\ d_\sigma^2$).

In the form of single crystals, this compound shows a first-order phase transition from LS to HS phases at thermal equilibrium[18,19]. Nano-crystals of this material dispersed in polymeric matrix lose the 1st order transition and show a more gradual spin conversion[16], as a result of both the pressure effects and anchoring processes (physisorption, capillarity) due to the polymers[20]. It was recently demonstrated by time-resolved studies that these Fe^{III} nanocrystals exhibit photo-switching toward a transient HS state by photo-excitation of the LS state[8a]. Here we present new results and detailed analysis of the spin state photo-switching dynamics by means of femtosecond pump-probe optical spectroscopy. It is easier to investigate an assembly of nano-crystals dispersed in a PVP polymer film than single crystals: the low optical density of the nano-crystals allows to perform a detailed study over a broad spectral range from UV to IR. Single crystals restrict the range of wavelengths for spectroscopic probing due to the higher optical density (OD)[8a,16a].

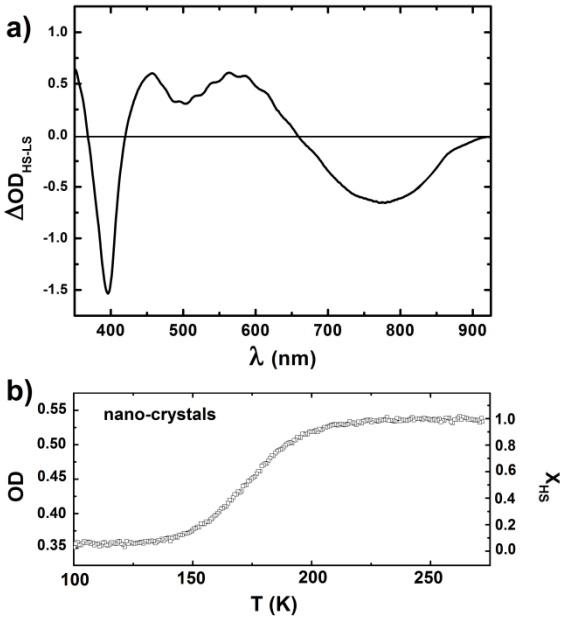

Fig.1 Difference of optical density in the (350-925 nm) spectral window between HS state (296 K) and LS state (16 K) measured on the nano-crystals sample (a). Photo-excitation is performed at 850 nm in the tail of the LS absorption band. OD at 550 nm (left axis) of the nano-crystal assembly during the crossover scaled to X_{HS} (right axis) (b).

Fig. 1 shows the variation of optical density *ΔOD* measured on the films of nano-crystals, between pure LS state (16 K) and pure HS state (296 K). It reveals phenolate-to-iron charge-transfer bands (CT) in the near-infrared (NIR) - visible (VIS) with distinct features for LS and HS states. With respect to that of LS state, the OD of the HS state is higher in VIS and lower in NIR parts of the spectrum, with a well-defined isosbestic point around 650 nm. The thermal fraction of HS molecules $X_{HS}(T)$ is obtained by scaling the change of optical density *OD(T)* at a given temperature *T* to the change of optical density between LS (OD_{LS}) and HS (OD_{HS}) states:

$$X_{HS}(T) = \frac{OD(T) - OD_{LS}}{\Delta OD_{HS-LS}}$$

The thermal behavior of $X_{HS}(T)$ obtained in this way is displayed in Fig. 3(b) and indicates a gradual conversion spanning from 140 K to 220 K, in agreement with magnetic measurements[16].

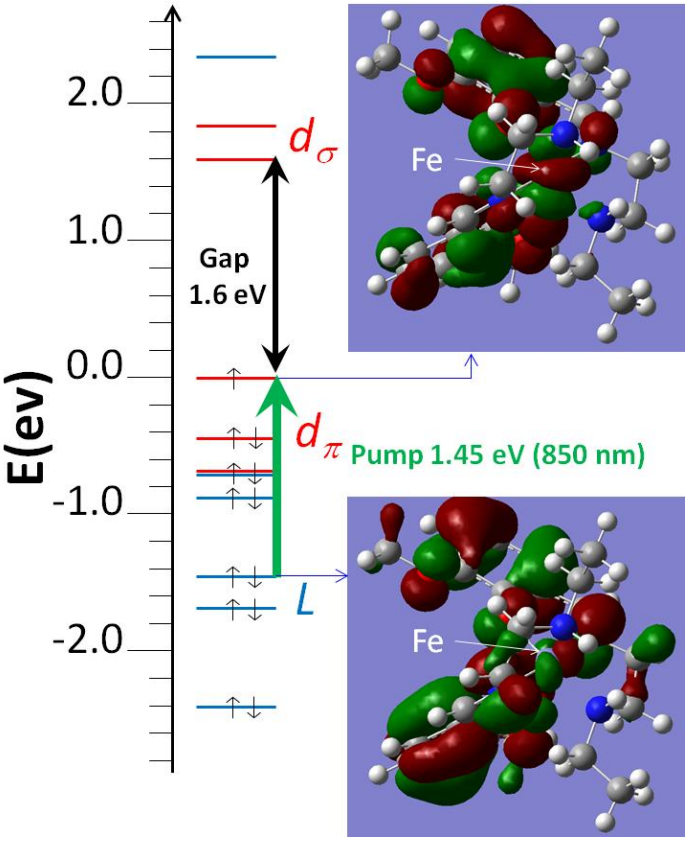

Fig. 2. LS schematic energy diagram and frontier molecular orbitals obtained from DFT calculations. Red: d_σ and d_π metal-like orbitals, blue : ligand-like orbitals. The HOMO-LUMO gap (1.6 eV) is larger than the pump excitation at 1.45 eV (850 nm). With respect to the HOMO (strong weight on a Fe d orbital), a few doubly occupied molecular orbitals (centered on phenol groups) falls within the energy range corresponding to the photo-excitation.

In the following, we exploit these spectroscopic fingerprints, to study the ultrafast spin-state photo-switching and the resulting energy dissipation into the material.

Inter-System Crossing and vibrational cooling

The spin-state photo-switching is known to proceed via transient intermediate states, as the direct low energy excitation from LS to HS state is forbidden by spin parity. In the case of Fe^{II} systems, the photo-switching at the molecular level results from the promotion by light of an electron from the metal center to the ligand orbitals (MLCT excited state). For this Fe^{III} $[Fe(3\text{-MeO-SalEen})_2]PF_6$ system, we performed DFT calculations with Gaussian 09 package to establish the molecular orbital energy diagram. Fig. 2 shows that in the LS state the highest occupied molecular orbital (HOMO) and lowest unoccupied molecular orbitals (LUMO), both of Fe d predominant character, are separated by a 1.6 eV energy gap. We found that the low energy excitation at 850 nm (1.45 eV) therefore may promote an electron from a few symmetry-adapted and doubly-occupied molecular orbitals (centered on the phenol group, noted *L*) to the HOMO with a strong weight on the d orbital of the metal center (*M*). This LMCT state corresponds then to a $L^1d_\pi^6d_\sigma^0$ electronic configurations.

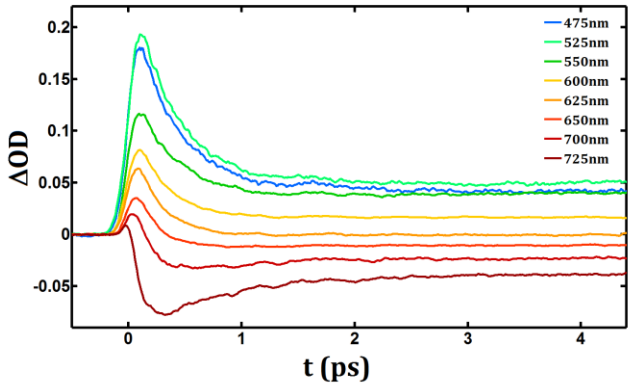

Fig. **3**. Change of optical density at different probe wavelengths after fs excitation at 850 nm measured on $[Fe^{III}(3\text{-MeO-SalEen})_2]PF_6$ nano-crystals**.** Measurements are performed at 100K in pure LS state.

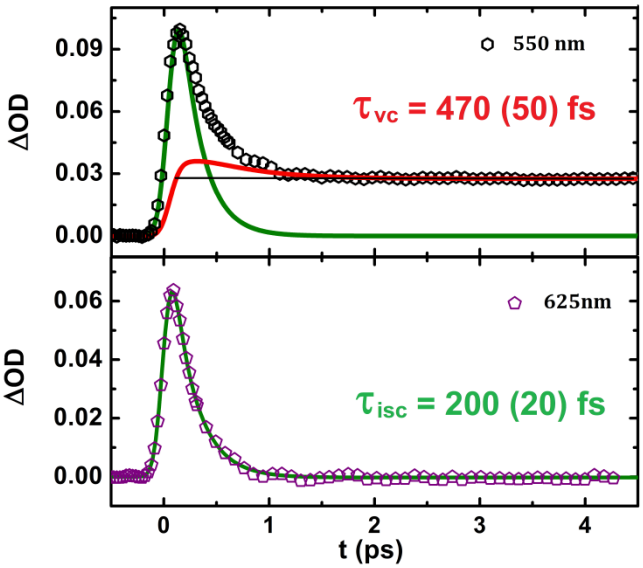

Fig. 4. Deconvolution of raw data into the relaxation kinetic of the INT electronic states ($\tau_{isc,}$, green line) and the population kinetic of the HS state taking into account vibrational cooling ($\tau_{vc,}$ red line). Only 1/8 of the experimental data are shown for clarity.

By using femtosecond optical spectroscopy (see experimental section), it is possible to study the photo-switching dynamics since the different molecular states have peculiar optical spectra (Fig. 1). Selected time traces of transient OD measurements performed at different probing wavelengths are plotted in Fig. 3-5. The OD increase in the VIS part and bleaching in the NIR part (at the ps timescale), are characteristic of the formation of the HS state, as observed during the thermal LS to HS conversion (Fig. 1) and previously reported on similar samples[8a,16].

Around time zero, the OD spectrum differs significantly from those of the LS ground state and of the HS photoinduced state, in terms of intensities or spectral range, where OD increases or decreases. This is the optical fingerprint of the LMCT state. The kinetic evolution of the optical density around the isosbestic point at 625 nm, where the OD of LS and photoinduced HS states are the same[8a], allows to selectively follow the dynamics of this intermediate (Franck-Condon) state.

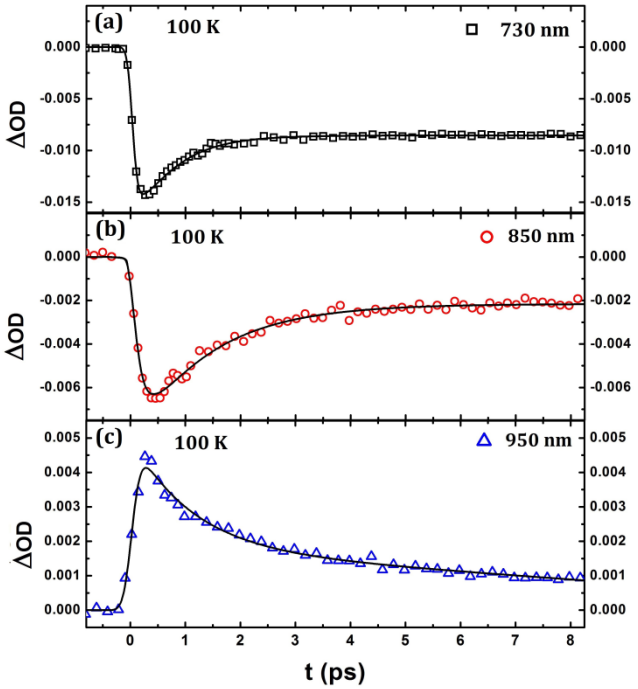

Fig. 5. Fit of the ΔOD traces at 730, 850 & 950 nm with bi-exponential functions describing ISC and vibrational cooling.

The OD kinetic trace at 625 nm shows at first a rapid rise (limited by our time resolution) corresponding to the generation of the LMCT state, which then decays towards the final HS state. Rigorously speaking, the dynamics may involve a sequence of transient states between LS and HS, as already reported in the case of Fe^{II} systems. But since we do not observe clear fingerprints of different intermediate states, we consider only a lump intermediate state (INT) including the LS LMCT state ($L^1d_\pi^6d_\sigma^0$ electronic configuration) and other possible intermediates, such as those resulting from $L^1d_\pi^5d_\sigma^1$ or $L^1d_\pi^4d_\sigma^2$ electronic configurations.

The inter-system crossing (ISC) sequence from LMCT to HS is well described at 625 nm by a single exponential decay. The fit shown in Fig. 4 gives τ_{ISC} = 200 ± 20 fs. For other measurements with probe wavelengths away from the isosbestic point, the single exponential model fails to reproduce the observed dynamics and slower components are observed on the ps time-scale, as shown at 550 nm for example. This is especially true in the IR region (950 nm, Fig. 5), more sensitive to vibrational cooling since lower energetic levels are probed. Thus we used a two-exponential decay model for fitting both dynamics, the first time constant describing the ISC being fixed to τ_{ISC} = 200 fs. Depending on the probe wavelength the vibrational cooling time constant τ_{VC} varies from 470 (50) fs at 550 nm and up to 1.6 (0.2) ps at 950 nm. At 730 and 850 nm the probe is sensitive both to vibrational cooling but also to LS state bleaching, thus making the interpretation more difficult. These measurements in the visible and infrared region reveal therefore that even if the system has reached the HS potential within ≈200 (20) fs, more than one picosecond is needed for the HS molecule to thermalize with its environment.

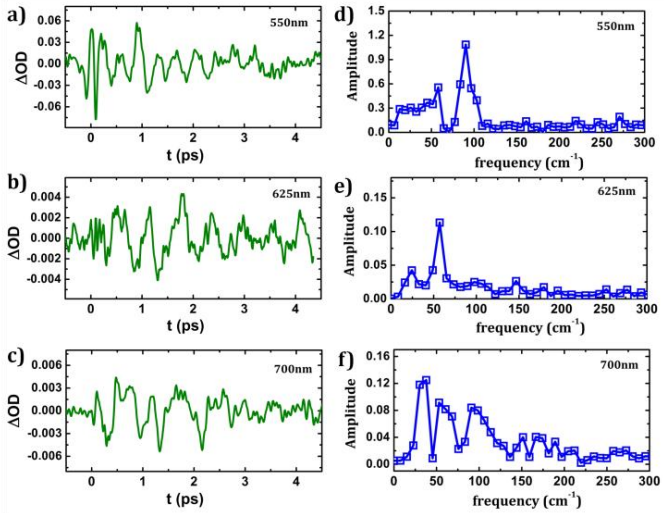

Fig. 6. (a-c), Oscillating component of OD at 550, 625, and 700 nm. (d-f) corresponding FFT of the experimental data, showing the activation of different modes around 85, 56 et 35 cm^{-1}.

The τ_{VC}≈1.6 ps observed here corresponds to the transfer of the excess energy deposited on the molecule by the laser to the lattice. This timescale is shorter than that reported for Fe^{II} molecules in solution (up to 10 ps) with infrared experiments[10,11]. This may be due to the fact that in crystals the excited molecules interact efficiently with the lattice system via phonon-phonon coupling.

Coherent structural oscillations

A closer inspection of the ΔOD time traces in Fig. 3-4 allows the observation of weak oscillating components. Fig. 6 (a-c) shows the deviation of the OD data from the exponential fits for different probe wavelengths. The corresponding Fourier transforms of the residual parts corresponding to positive delay are presented in Fig. 6 (d-f). At 550 nm, a prevailing mode is observed around 85 cm^{-1} (similar oscillations are observed at 525 and 475 nm in Fig. 3). At the wavelength on the isobestic point (625 nm) another mode is observed around 56 cm^{-1}. These modes are equally observed at 700 nm, where a third mode around 35 cm^{-1} also appears.

A similar vibrational coherence in the photoinduced high-spin state was reported for Fe^{II} SCO molecules in solution[21] and more recently in $[Fe(phen)_2(NCS)_2]$ crystals[14]. The mechanism behind the high quantum efficiency of LIESST in Fe^{II} SCO compounds was theoretically proposed to result from the instantaneous coupling of the excited (MLCT) state with the phonons of the final (HS) state[13]. The first experimental proof of this process was provided by femtosecond optical pump-probe spectroscopy studies of LIESST in $[Fe(phen)_2(NCS)_2]$ crystals, where the breathing mode (113 cm^{-1}) associated with the elongation of the Fe-N bonds was clearly identified[14]: the instantaneous activation of this molecular breathing phonon drives the system from the MLCT to the HS potential within 170 fs, i.e. on the timescale of a half period of such molecular vibration. The fast damping of the key molecular phonon modes leads to the efficient trapping the HS state. It may also result from intermolecular contacts.

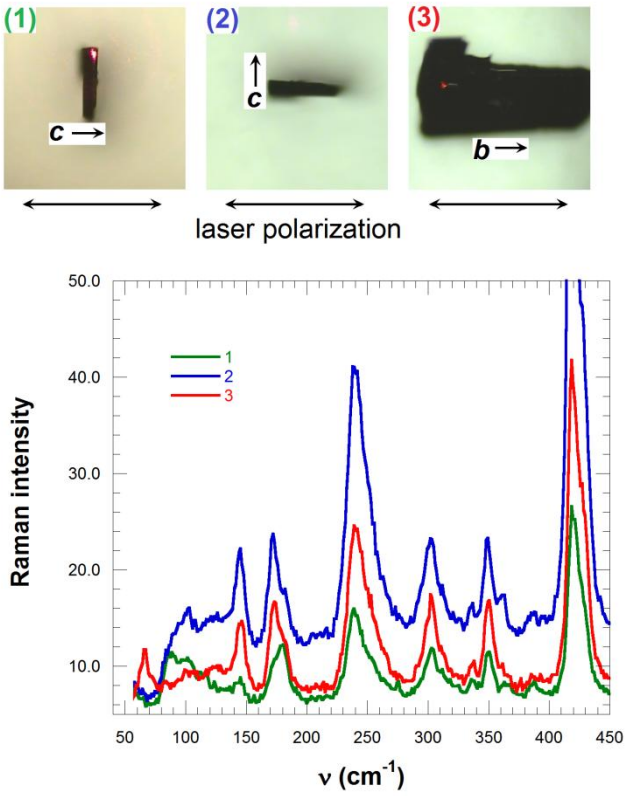

Fig. 7. Raman spectra obtained on single crystals for different polarization (1), (2) and (3) shown in the photographs on the top.

The present observation of the activation of such coherent structural vibrations during LIESST in Fe^{III} SCO crystals may therefore be also attributed to such mechanism. However, there are very few vibrational spectroscopy studies of Fe^{III} compounds in literature, even though these low frequencies vibrations are often attributed to ligand breathing or torsion modes[22]. We thus performed Raman measurements at room temperature, as well as calculations of molecular vibrations on the $[Fe(3\text{-}MeO\text{-}SalEen)]PF_6$ compound for gaining insights on the frequencies and nature of such modes.

Raman and DFT studies of the HS phase

We used a single crystal for finding the crystal axis orientation with x-ray diffraction and checking polarization effect on Raman signal. Fig. 7 shows the single crystal Raman spectra obtained at room temperature. Since the crystalline space group is $P_{\bar{1}}$ and the molecules are in general positions in the unit cell[16a], the modes split in two categories: the totally symmetric ones (A_g and Raman active) where molecules oscillate in phase with respect to inversion symmetry and the antisymmetric ones (A_u and IR active). The Raman spectra reveal several low frequency modes, especially around 65, 85, 100, 145, 172, 181, 240 and 260 cm^{-1}. In this frequency range, the modes may be the skeletal modes of the $[FeN_4O_2]$ core, but may also correspond to ligand distortions. Because of the C_i point symmetry of the crystal, there is no polarization selection: only the Raman intensity may depend on the sample orientation with respect to the laser polarization.

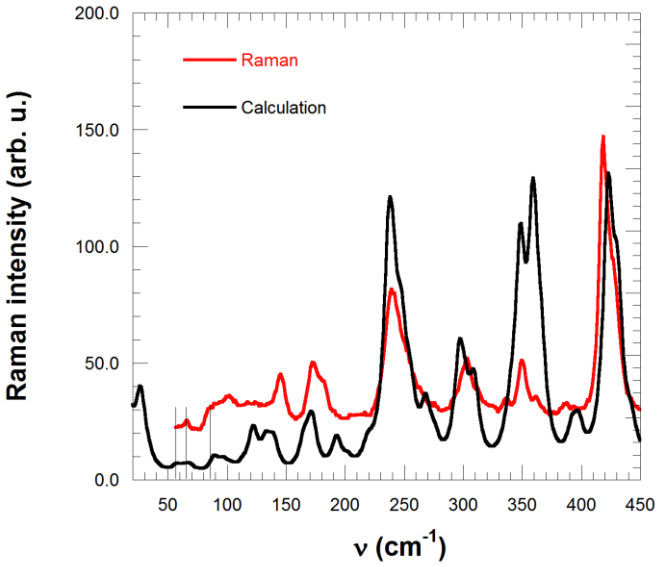

Fig. 8. Comparison of the calculated and experimental (averaged of the different polarizations) Raman spectra.

According to Fig. 7 the relative intensity of the different modes changes with sample orientation. The Raman mode around 85 cm^{-1} corresponds well to the coherent vibration observed during LIESST in the present Fe^{III} compound. The modes at 35 and 56 cm^{-1} could not be measured with our Raman set-up because of the dielectric edge filter cut-off.

For understanding better the nature of the molecular vibrations involved during LIESST, we carried out molecular vibration frequencies calculations with DFT methods for an isolated $[Fe(3\text{-}MeO\text{-}SalEen)_2]PF_6$ complex, after geometry optimization, by using hybrid B3LYP functional with triple-ζ 6-311g(d,p) basis set within Gaussian09 code[23,24]. In Fig. 8 we compare the calculated Raman spectrum with the experimental results from Fig. 7, averaged over the different orientations measured on a single crystal for better comparison with calculations. The overall calculations reproduce quite well the observed Raman spectrum. A complete analysis of the modes and the nature of the vibrations will be published elsewhere and in this paper we focus on the modes observed with time-resolved spectroscopy. In the low frequency region, the calculated modes at 88, 56 and 33 cm^{-1} are close to those observed by Raman and/or time-resolved spectroscopy. The mode at 56 cm^{-1} (shown in video S1) is mainly associated with Fe-N breathing of the FeN_4O_2 coordination sphere. The modes at 33cm^{-1} (video S2) and 88 cm^{-1} (video S3) are mainly ligand torsion modes. Since during the LS to HS conversion the structural reorganization involves both the molecular breathing (as Fe-L bonds elongate) and the ligand torsion, such modes should play an important role during the self-trapping process.

For understanding why different vibration modes are observed during LIESST depending on the probe wavelength, we need to analyze optical absorption of HS species through an accurate description of excited states and a time dependent DFT (TD-DFT) approach is required[25].

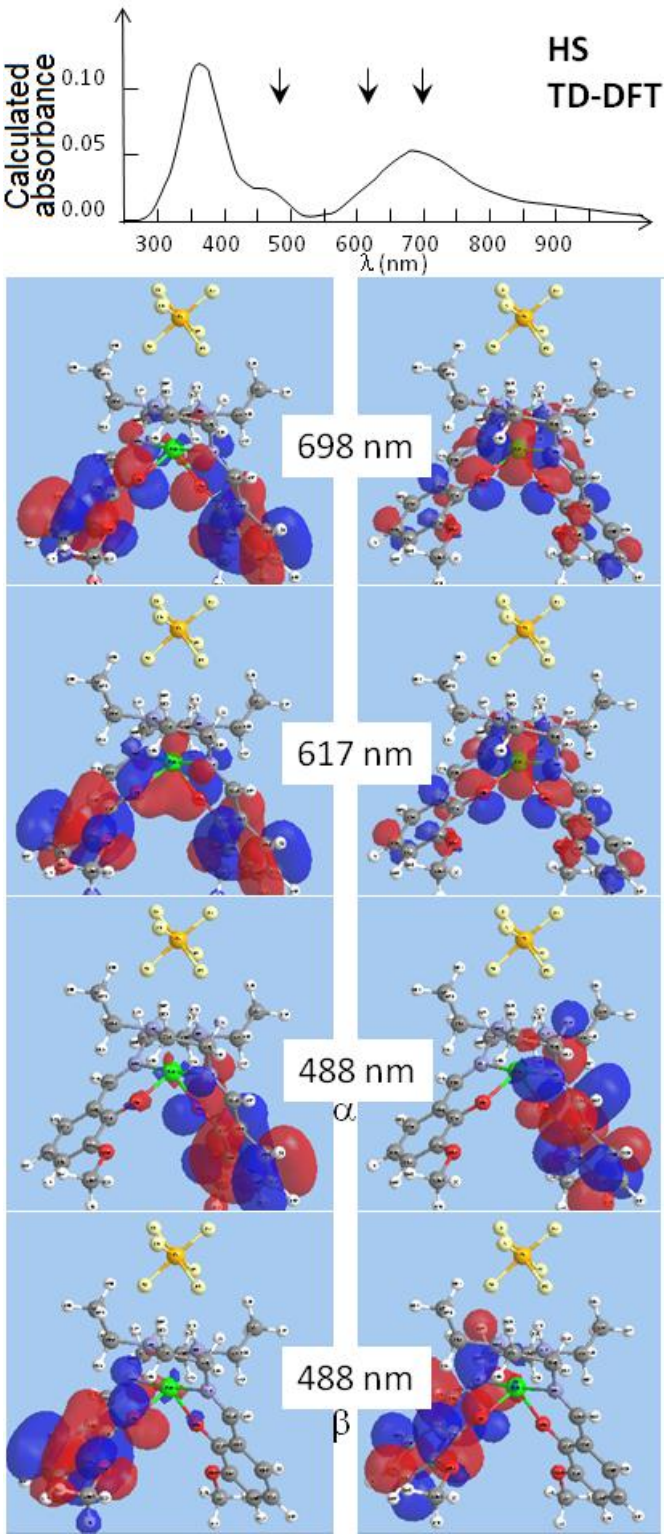

Fig. 9. Natural transition orbitals of hole (left) and particle (right) calculated in the case of HS species at 698, 617 and 488 nm, i.e. close to the experimental probes at 700, 625 and 550-475 nm. α and β designate spin ↑ and spin ↓. The calculated absorbance spectrum (top) underline the strong weight of these transitions.

The obtained natural transition orbitals (NTO) taking into account the hole–particle pairs resulting from light absorption can then be used to interpret our data.

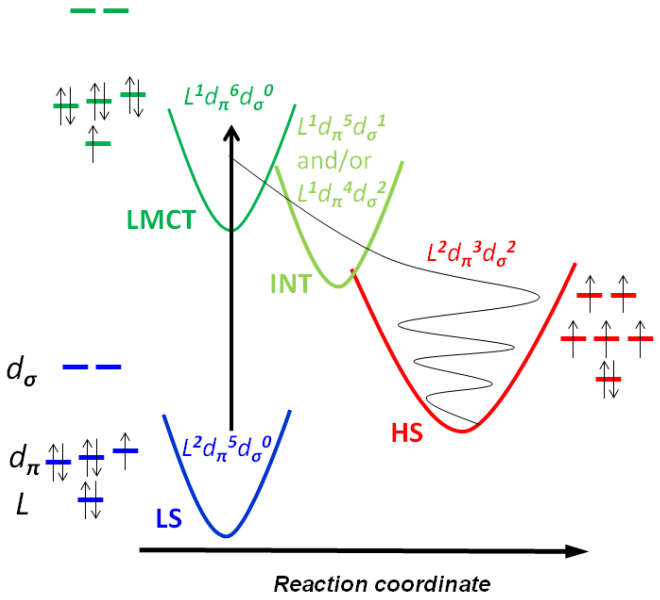

Fig. 10. Schematic representation of the photoswitching trajectory along a simple reaction coordinate.

Fig. 9 shows the NTO corresponding to the hole–particle transition state around 500, 617 and 700 nm. The strong weight of the particle orbital on the Fe-N (and Fe-O) bonds for the transition at 617 nm explains the sensitivity to the breathing mode of the pump-probe data at 625 nm. The transition state around 700 or 500 nm are characterized by a strong weight of the particle orbital mainly located on one ligand and explain the sensitivity to ligand torsion.

Ultrafast LIESST dynamics in Fe^{III} systems

Our investigation gives important insights on the ultrafast mechanism of LIESST in a Fe^{III} system, schematically represented in Fig. 10. Molecular orbital calculations (Fig. 2) indicate that the photo-excitation of the LS ($L^2d_\pi{}^5d_\sigma{}^0$) generates a LMCT state ($L^1d_\pi{}^6d_\sigma{}^0$). Time-resolved spectroscopy data show that the LMCT state decays to the HS state ($L^2d_\pi{}^3d_\sigma{}^2$), possibly through other intermediate electronic states such as $L^1d_\pi{}^5d_\sigma{}^1$ or $L^1d_\pi{}^4d_\sigma{}^2$. However, since the HS potential is reached within ≈200 fs, these electronic states only serve as mediators and are dynamically mixed. The different photoexcited molecules arrive "simultaneously" on the HS potential, where they oscillate. The global coherent oscillations experimentally observed underline that the phase is mainly kept between the different photo-excited molecules. Indeed, the observation of vibrational coherence in the photoinduced HS state with oscillation around 85 cm^{-1} (392 fs period), requires that the photoexcited molecules reach the HS potential on a timescale shorter than a half oscillation period to avoid dephasing. This is in agreement with τ_{ISC} = 200 ± 20 fs observed by time-resolved spectroscopy (Fig. 4). This very short time-scale is similar to the one reported for LIESST in Fe^{II} SCO systems[10,14] and also indicates that intermediates other than LMCT and HS states mainly serve as mediators.

The instantaneous activation of several phonons of the HS state results from the important displacive nature of the mechanism. However, the structural change between LS and HS structures involves several degrees of freedom such as molecular breathing, torsion..., which may be activated with different timescales. Therefore, the transformation pathway connecting the initial photo-excited state to the photoinduced HS state is only roughly described by the classical single coordinate picture employed here in Fig. 10. A more complex multi-dimensional energy surface description has to be used for a more detailed analysis. However, these results indicate that on such short time-scale the wave functions describing the electronic and structural degrees of freedom are strongly coupled during the process. This LS-to-HS photoswitching dynamics is therefore very different in nature from the reverse HS-to-LS one observed recently in a Fe^{II} SCO material, where a true (vibrationally cooled) triplet state is populated and depopulated within 10's ps[9]. Indeed, such slow reverse-LIESST dynamics obey the Born-Oppenheimer approximation.

Local nature of ultrafast LIESST

Another important question associated with LIESST in crystals is the possibility of cooperative response to light excitation. We look into possible cooperativity on ps timescale by following the fraction ΔX_{HS} of molecules converted after 5 ps from LS to HS state. It is monitored by femtosecond optical spectroscopy for different excitation densities and for different temperature (and therefore different initial fractions of molecules in LS states as shown in Fig. 1). Fig. 11 shows how ΔX_{HS} changes with the pump laser fluence F (i.e. on the excitation density). It is clear that ΔX_{HS} depends linearly on F, i.e. there is no amplification on such ultra-short time scale. The observed slopes in Fig. 11 correspond to the photo-response and are given here in $\Delta X_{HS}/F$. The slopes measured for different temperatures, proportional to the number of photo-switched molecules per incident photon, change with temperature. This is not surprising because the fraction of molecules in the LS state decreases above 120 K (Fig. 1). Therefore the fraction of molecules switched from LS to HS states, should be weighted both by X_{LS}, the initial fraction of molecules in the LS state at a given temperature ($X_{LS} = 1-X_{HS}$), and by the laser fluence F.

$$\Delta X_{HS} \propto F \times X_{LS} \text{ or } \Delta X_{HS} / F \propto X_{LS}$$

Fig 11(b) shows that the photo-response $\Delta X_{HS}/F$ depends linearly on X_{LS}. Incidentally, based on such plot we can also conclude on the absence of back conversion with the same pump wavelength (from HS to LS), since in such a case the photo-response would be negative as X_{LS} will tend to 0. These important results underline the local nature of the photo-switching process occurring within a picosecond. Each individual photo-switching process can be regarded as an isolated molecular event. It is only on longer time-scale that macroscopic conversion occur, driven by elastic and thermal mechanisms[18].

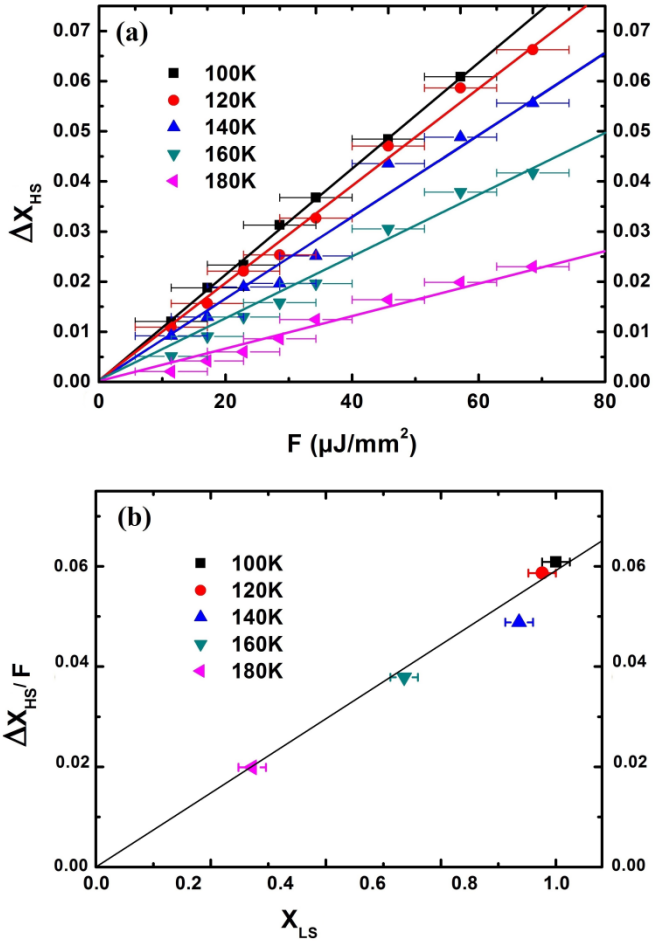

Fig. 11. (a) Temperature dependence of the fraction of molecules photo-switched to the HS state (ΔX_{HS}) for different pump fluencies. (b) Dependence of the photo-response ($\Delta X_{HS}/F$) with the initial fraction of LS molecules (X_{LS}).

Conclusions

This detailed study allows to draw a complete picture of the LIESST photo-switching process in Fe^{III} systems in the solid state. First of all, the photo-response is local on ps timescale, as characterized by the linear dependence with the number of photons and with the initial fraction of molecules in the LS state. This confirms that the initial mechanism might be seen as a local molecular event. Our new data in the present Fe^{III} system also reveal that during the LIESST process several key modes are coherently activated. They are associated with changes of relevant reaction coordinates accompanying change of spin state (breathing, torsion...). The Fe-N lengthening is shorter in Fe^{III} (0.15 Å) than in Fe^{II} (0.20 Å) and the frequency of the breathing modes differ. If a clear breathing mode (in phase elongation of the 6 Fe-N bonds) is easily identified in $Fe^{II}N_6$ systems (around 113 cm^{-1})[14] the lower symmetry of the present compound with $Fe^{III}N_4O_2$ coordination sphere makes such identification more difficult and several modes may involve Fe-N elongation (as it is the case of the 56 cm^{-1} mode). In addition, the breathing frequencies depend on the ligand (mass) and on the strength

of its bonding to the metal. However, our results indicate that the mechanism behind the ultrafast intersystem crossing in Fe^{II} and other transition-metal complexes[13,14], described in terms of the dephasing of the photoexcited state to the phonon continuum of the photoinduced (here HS) state with significantly different structure, is also valid for describing the photo-switching mechanism in Fe^{III} systems. The observed structural coherence underlines the dynamical nature of the light-induced excited spin-state trapping process, as opposed to the so far prevailing kinetic description based on simple exponential decay from photo-excited to photoinduced states.

Experimental

Sample preparation

The molecular compound $[Fe(3\text{-}MeO\text{-}SalEen)_2]PF_6$ was synthesized in the form of a microcrystalline powder and single-crystals as previously described[16a,18]. Nanocrystals[16c] were prepared by rapidly adding a concentrated solution of salt (10 mg) in acetone (1 mL) into a large volume (20 mL) of butan-1-ol maintained at -40 °C under a vigorous stirring. After 15 minutes, the particles were isolated by centrifugation, rinsed with pentane, dried. The properties of needle-shaped nanocrystals (typical dimensions of 900(230)x285(65)x64(18) nm^3 from TEM) were checked with powder X-ray diffraction, IR and magnetism[16c]. The nanocrystals were processed in PVP polymeric films. 5 mg of nanocrystals were added to a viscous solution of 100 mg of PVP (MM = 45000 $gmol^{-1}$) in 500 µL of butan-1-ol ; the mixture was sonicated (30 min), then spin-coated on glass substrates (1000 rpm) and dried at air before use.

Femtosecond optical spectroscopy

For tracking the photo-induced spin state switching dynamics in real time, we employ femtosecond pump probe transmission measurements[17a]. The laser beam was provided from the output of a femtosecond regenerative amplifier (Legend Elite, Coherent) and then split in two beams, each of them seeding an optical parametric amplifier (TOPAS, Light Conversion) allowing to cover spectral range from UV to infrared. The experimental time resolution is 140 fs. The pump wavelength was set at 850 nm corresponding to the LMCT absorption band. The photo-excited HS state relaxes towards the LS state in less than 1 ms, allowing the 1 kHz repetition rate of the experiment. The sample was cooled down using a nitrogen cryostream. The one colour probe beam, tuned across a broad spectral range (480-950 nm) measured transient optical density. We could measure the variation of the fraction of HS molecules $\Delta X_{HS}(t)$ by scaling $\Delta OD(t)$, the change of OD in time between LS and photo-excited HS state, to the OD change between LS and HS states at thermal equilibrium.

Raman spectroscopy

Raman spectra were collected in the 55-1200 cm^{-1} low frequency range using a LabRAM-HR Raman spectrometer (Horiba / Jobin Yvon). A $100\times300\times30\mu m^3$ single crystal has been studied for different polarisation configurations. The 632.818 nm line of a 15 mW He-Ne laser was used as the excitation source. The exciting radiation was directed through a neutral density filter (optical density 2) to avoid sample heating problems and was focused on the sample via a x100 long working-distance objective. The scattered light was collected in backscattering configuration and the Rayleigh scattering was removed by means of a dielectric edge filter.

DFT calculations

Molecular vibration frequencies calculations were carried out for $[Fe(3\text{-}MeO\text{-}SalEen)]PF_6$ after geometry optimization, by using hybrid B3LYP functional with triple-ζ 6-311g(d,p) basis set within Gaussian09 code[23]. Frequencies are determined from the second derivatives of the energy with respect to the atomic positions and then operating transformation to mass-weighted coordinates. Exploring the results especially for the vibrations and their animations with screen captures was done with Gaussview annex module to Gaussian.

TD-DFT as implemented in the Gaussian 09 package[23] was applied for obtaining the NTO of the HS $[Fe(3\text{-}MeO\text{-}SalEen)]PF_6$ system, starting from preliminary geometry optimized molecule with B3LYP/6-311g(*d,p*) functional-basis set.

Acknowledgements

This work was supported by the Institut Universitaire de France, Rennes Métropole, Région Bretagne (CREATE 4146), ANR (ANR-13-BS04-0002) and Fonds Européen de Développement Régional (FEDER). Raman measurements have been performed on the SIR raman system from the ScanMAT platform of Rennes 1 University.

Notes and references

1 a) D. Polli, P. Altoe, O. Weingart, K.M. Spillane, C. Manzoni, D. Brida, G. Tomasello, G. Orlandi, P. Kukura, R.A. Mathies, M. Garavelli, and G. Cerullo, *Nature*, 2010, **467**, 440-443; b) A. H. Zewail. *Angew. Chem. Int. Ed*. 2000, **39**, 2586-2631; c) J.H Lee, M. Wulff, S. Bratos, J. Petersen, L. Guérin, J.C Leiknman, M. Cammarata, Q.Y. Kong, J. Kim, K. Moller, and H.J. Hee, *J. Am. Chem. Soc.*, 2013, **135**, 3255.

2 a) M. Gao, C. Lu,H. Jean-Ruel, L. C. Liu, A. Marx, K. Onda, S. Koshihara, Y. Nakano, X. Shao, T. Hiramatsu, G. Saito, H. Yamochi, R. R. Cooney, G. Moriena, G. Sciaini, and R.J.D. Miller, *Nature,* 2013, **496**, 343-346; b) T. Ishikawa, N. Fukazawa, Y. Matsubara, R. Nakajima, K. Onda, Y. Okimoto, S. Koshihara, M. Lorenc, E. Collet, M. Tamura and R. Kato, *Physical Review B*, 2009, **80**, 115108; c) Y. Kawakami, S. Iwai, T. Fukatsu, M. Miura, N. Yoneyama, T. Sasaki, and N. Kobayashi, *Phys. Rev. Lett*., 2009, **103**, 066403.

3 a) H. Okamoto, Y. Ishige, S. Tanaka, H. Kishida, S. Iwai, and Y. Tokura, *Phys. Rev. B*, 2004, **70**, 165202; b) L. Guérin, J. Hébert, M. Buron-Le Cointe, S. Adachi, S. Koshihara, H. Cailleau, and E. Collet, *Phys. Rev. Lett*., 2010, **105**, 246101.

4 M. Halcrow, Ed., Spin-crossover materials (Wiley, West Sussex, 2013) ISBN 9781119998679.

5 a) S. Decurtins, P. Gütlich, C.P. Köhler, H. Spiering, and A. Hauser, *Chem. Phys. Lett.*, 1984, **105**, 1; b) A. Hauser, *Chem. Phys. Lett.*, 1992, **192**, 65-70.

6 J.F. Létard, L. Capes, G. Chastanet, N. Moliner, S. Létard, J.A. Real, and O. Kahn, *Chem. Phys. Lett.*, 1999, **313**, 115.

7 a) N. Bréfuel , H. Watanabe, L. Toupet, J. Come, N. Matsumoto, E. Collet, K. Tanaka and J.-P. Tuchagues, *Ang. Chem. Int. Ed.*, 2009, **48**, 304-9307; b) E. Collet, H. Watanabe, N. Bréfuel, L. Palatinus, L. Roudaut, L. Toupet, K. Tanaka, J.-P. Tuchagues, P. Fertey, S. Ravy, B. Toudic, and H. Cailleau, *Phys. Rev. Lett.*, 2012, **109**, 257206.

8 a) R. Bertoni, M. Lorenc, A. Tissot, M. Servol, M.-L. Boillot, and E. Collet, *Angew. Chem. Int. Ed.*, 2012, **51**, 7485-7489; b) W. Kaszub, A. Marino, M. Lorenc, E. Collet, E.G. Bagryanskaya, E.V. Tretyakov, V.I. Ovcharenko and M.V. Fedin, *Ang. Chem. Int. Ed.*, 2014, **53**, 10636-10640; c) A. Marino, M. Buron-Le Cointe, M. Lorenc, L. Toupet, R. Henning, A.D. DiChiara, K. Moffat, N. Bréfuel, E. Collet, *Faraday Discussion*, 2015, **177**, 363-379.

9 A. Marino, P. Chakraborty, M. Servol, M. Lorenc, E. Collet and A. Hauser, *Ang. Chem. Int. Ed.*, 2014, **53**, 3863-3867.

10 a) W.Gawelda, A. Cannizzo, V.T. Pham, F. van Mourik, C. Bressler, and M. Chergui, *J. Am. Chem. Soc.*, 2007, **129**, 8199–8206; b) A. Canizzo , C. Milne, C. Consani, W. Gawelda, C. Bressler, F. van Mourik, and M. Chergui, *Coord. Chem. Rev.*, 2010, **254**, 2677-2686; c) J.K. McCusker, K.N. Walde, R.C Dunn, J.D Simon, D. Madge, and D.N. Hendrickson, *J. Am. Chem. Soc.*, 1992, **114**, 6919-6921; d) J.E. Monat, and J.K. McCusker, *J. Am. Chem. Soc*., 2000, **122**, 4092-4097; e) A.L. Smeigh, M. Creelman, R.A. Mathies, and J.K. McCusker, *J. Am. Chem. Soc.*, 2008, **130**, 14105-14107; f) M. M. N. Wolf, R. Groß, C. Schumann, J. A. Wolny, V. Schünemann, A. Døssing, H. Paulsen, J. J. McGarvey, and R. Diller, *Phys. Chem. Chem. Phys*., 2008, **10**, 4264–4273; g) I. Lawthers, and J. J. McGarvey, *J. Am. Chem. Soc*., 1984, **15**, 106.

11 a) C. Bressler, C. Milne, V.-T. Pham, A. El Nahhas, R. M. van der Veen, W. Gawelda, S. Johnson, P. Beaud, D. Grolimund, M. Kaiser, C. N. Borca, G. Ingold, R. Abela and M. Chergui, *Science*, 2009, **323**, 489; b) N. Huse, H. Cho, K. Hong, L. Jamula, F.M.F. de Groot, T.K. Kim, J.K. McCusker, and R.W. Schoenlein, *J. Phys. Chem. Lett*., 2011, **2**, 880-884; c) M. Khalil, M. M. Marcus, A. L. Smeigh, J. K. McCusker, H. H. W. Chong and R. W. Schoenlein, *J. Phys. Chem. A.*, 2006, **110**, 38; d) W. Gawelda, V.-T. Pham, M. Benfatto, Y. Zaushitsyn, M. Kaiser, D. Grolimund, S. L. Johnson, R. Abela, A. Hauser, C. Bressler and M. Chergui, *Phys. Rev. Lett.*, 2007, **98**, 057401; e) S. Nozawa, T. Sato, M. Chollet, K. Ichiyanagi, A. Tomita, H. Fujii, S.-I. Adachi and S.-Y. Koshihara, *J. Am. Chem. Soc.*, 2010, **132**, 61; f) H.T. Lemke, C. Bressler, L.X Chen, D.M. Fritz, K.J. Gaffney, A. Galler, W. Gawelda, K. Haldrup, R.W. Hartsock, H. Ihee, J. Kim, K.H. Kim, J.H Lee, M.M. Nielsen, A.B. Stickrath, W. Zhang, D. Zhu, and M. Cammarata, *J. Phys. Chem. A*, 2013, **117**, 735-740.

12 W. Zhang, R. Alonso-Mori, U. Bergmann, C. Bressler, M. Chollet, A. Galler, W. Gawelda, R. G. Hadt, R. W. Hartsock, T. Kroll, K. S. Kjær, K. Kubiček, H. T. Lemke, H. W. Liang, D. A. Meyer, M. M. Nielsen, C. Purser, J. S. Robinson, E. I. Solomon, Z. Sun, D. Sokaras, T. B. van Driel, G. Vankó, T.-C. Weng, D. Zhu and K. J. Gaffney *Nature*, 2014, **509**,345–348.

13 a) M. Van Veenendaal, J. Chang, and A.J. Fedro, *Phys. Rev. Lett.*, 2010 **104**, 067401; b) J. Chuang, A.J. Fedro, and M. Van Veenendaal, *Phys. Rev. B*, 2010, **82**, 075124.

14 a) M. Cammarata, R. Bertoni, M. Lorenc, H. Cailleau, S. Di Matteo, C. Mauriac, S. F. Matar, H. Lemke, M. Chollet, S. Ravy, C. Laulhé, J.-F. Létard and E. Collet**,** *Phys. Rev. Lett*., 2014, **113**, 227402; b) R. Bertoni, M. Cammarata, M. Lorenc, S. F. Matar, J.-F. Létard, H. T. Lemke and E. Collet *Acc. Chem. Res.*, 2014, DOI: 10.1021/ar500444d

15 a) S. Hayami, Z. Gu, M. Shiro, Y. Einaga, A. Fujishima and O. Sato, *J. Am. Chem. Soc.* 2000, **122**, 7126 –7127; b) S. Hayami, K. Hiki, T. Kawahara, Y. Maeda, D. Urakami, K. Inoue, M. Ohama, S. Kawata and O. Sato, *Chem. Eur. J.*, 2009, **15**, 3497–3508; c) T. Shimizu, Y. Komatsu, H. Kamihata, Y. H. Lee, A. Fuyuhiro, S. Iijima and S. Hayami, *J. Inclusion Phenom. Macrocyclic. Chem.*, 2011, **71**, 363–369; d) G. Juhasz, S. Hayami, O. Sato and Y. Maeda, *Chem. Phys. Lett.*, 2002, **364**, 164–170; e) H. Ando, Y. Nakao, H. Sato and S. Sakaki, *J. Phys. Chem. A*, 2007, **111**, 5515 –5522; f) K. D. Murnaghan, C. Carbonera, L. Toupet, M. Griffin, M. M. Dîrtu, C. Desplanches, Y. Garcia, E. Collet, J.F. Létard and G. G. Morgan, *Chem. Eur. J.*, 2014, **20**, 5613-5618.

16 a) A. Tissot, R. Bertoni, E. Collet, L. Toupet, and M.-L. Boillot, *J. Mat. Chem.*, 2011, **21**, 18347-18353; b) R. Bertoni, M. Lorenc, A. Tissot, M.-L. Boillot and E. Collet, *Coord. Chem. Rev*., 2015, **282-283**, 66-76; c) A. Tissot, L. Rechignat, A. Bousseksou, and M.-L. Boillot, *J. Mater. Chem*. 2012, **22**, 3411-3419.

17 a) M. Lorenc, C. Balde, W. Kaszub, A. Tissot, Moisan, M. Servol, M. Buron-Le Cointe, H. Cailleau, P. Chasle, P. Czarnecki, M. L. Boillot and E. Collet, *Phys. Rev. B.*, 2012, **85**, 054302; b) H. Cailleau, M. Lorenc, L. Guérin, M. Servol, E. Collet and M. Buron-Le Cointe, *Acta Cryst. A*, 2010, **66**, 189; c) E. Collet, M. Lorenc, M. Cammarata, L. Guérin, M. Servol, A. Tissot, M.L. Boillot, H. Cailleau and M. Buron, *Chem. Eur. J.*, 2012, **18**, 2051 d) E. Collet, N. Moisan, C. Baldé, R. Bertoni, E. Trzop, C. Laulhé, M. Lorenc, M. Servol, H. Cailleau, A. Tissot, M.L. Boillot, T. Graber, R. Henning, P. Coppens and M. Buron, *Phys. Chem. Chem. Phys.*, 2012, **14** 6192.

18 M.S. Haddad, M.W. Lunch, W.D. Federer, and D.N. Hendrickson, *Inorg.Chem*., 1981, **20**, 123-131.

19 M. Sorai, R. Burriel, E. F. Westrum, and D.N. Hendrickson, *J.Phys. Chem. B*, 2008, **112**, 4344.

20 a) A. Tissot, C. Enachescu and M.-L. Boillot, *J. Mater. Chem*., 2012, **22**, 20451–20457; b) R. Tanasa, J. Laisney, A. Stancu, M.-L. Boillot and C. Enachescu, *Appl. Phys. Lett*., 2014, **104**, 031909.

21 C. Consani, M. Prémont-Schwarz, A. Elnahhas, C. Bressler, F. van Mourik, A. Cannizzo and M. Chergui, *Angew. Chem.* 2009, **121**, 7320.

22 M. Sorai, R. Burriel, E. F. Westrum, and D.N. Hendrickson, *J. Phys. Chem. B*, 2008, **112**, 4344.

23 M. J. Frisch *et al*, GAUSSIAN03 (revision C.02), Gaussian, Inc., Wallingford CT, 2004.

24 M. P. Andersson and P. Uvdal, *J. Phys. Chem. A*, 2005, **109**, 2937-2941

25 R. Martin, *J. Chem. Phys.* 2003, **118**, 4775